

Numerical solutions for a class of singular boundary value problems arising in the theory of epitaxial growth

Amit Kumar Verma^a, Biswajit Pandit^{b*}

^{a,b}*Department of Mathematics, Indian Institute of Technology Patna, Patna-801106, Bihar, India.*

Carlos Escudero^{c†}

^c*Departamento de Matemáticas & ICMAT (CSIC-UAM-UC3M-UCM),
Universidad Autónoma de Madrid, E-28049 Madrid, Spain.*

November 14, 2019

Abstract

The existence of numerical solutions to a fourth order singular boundary value problem arising in the theory of epitaxial growth is studied. An iterative numerical method is applied on a second order nonlinear singular boundary value problem which is the exact result of the reduction of this fourth order singular boundary value problem. It turns out that the existence or nonexistence of numerical solutions fully depends on the value of a parameter. We show that numerical solutions exist for small positive values of this parameter. For large positive values of the parameter, we find nonexistence of solutions. We also observe existence of solutions for negative values of the parameter and determine the range of parameter values which separates existence and nonexistence of solutions. This parameter has a clear physical meaning as it describes the rate at which new material is deposited onto the system. This fact allows us to interpret the physical significance of our results.

Keywords: Singular boundary value problems, epitaxial growth, non-self-adjoint operator, iterative numerical approximations.

1 Introduction

Along the years, a revolution of semiconductor device design has been spawned by the invention of superlattices and similar structures. These structures led to an improvement in the performances of many electronic instruments like lasers, diodes and bipolar transistors. Such advanced structures can be produced by means of epitaxial growth techniques. Epitaxial growth techniques that produce thin films under high vacuum conditions ([3]) have largely superseded older technologies in the semiconductor industry. Due to this success of epitaxial growth techniques, several mathematical models have been introduced in order to understand them better. In general terms, one could say that these models belong to one of two different classes: they are either discrete probabilistic models, such as cellular automata, or differential equations ([3]). In this work we strictly focus on the second type of model, and in particular we restrict our attention to the differential equation described in ([4, 8, 9, 7]). In these references the mathematical description of epitaxial growth is carried out by means of a function,

$$\sigma : \Omega \subset \mathbb{R}^2 \times \mathbb{R}^+ \rightarrow \mathbb{R}, \quad (1)$$

which describes the height of the growing interface in the spatial point $x \in \Omega \subset \mathbb{R}^2$ at time $t \in \mathbb{R}^+$. This function obeys the fourth order partial differential equation ([4])

$$\partial_t \sigma + \Delta^2 \sigma = \det(D^2 \sigma) + \lambda \Gamma(x, t), \quad x \in \Omega \subset \mathbb{R}^2, \quad (2)$$

where $\Gamma(x, t)$ models the incoming mass entering the system through epitaxial deposition and λ measures the intensity of this flux. Roughly speaking, the thin film grows by the introduction of new mass into the system (modeled by $\lambda \Gamma(x, t)$) and its structure is characterized by means of its height $\sigma(x, t)$. A basic modeling assumption is that this structure is dominated by processes taking place at the surface of the thin film which are

*Email: ^aakverma@iitp.ac.in, ^bbiswajitpandit82@gmail.com

†Email: ^ccel@icmat.es

coarse-grained modeled by the biharmonic operator and the nonlinearity. For simplicity we will focus on the stationary counterpart of this partial differential equation:

$$\Delta^2 \sigma = \det(D^2 \sigma) + \lambda G(x), \quad x \in \Omega \subset \mathbb{R}^2, \quad (3)$$

where we have assumed that $\Gamma(x, t) \equiv G(x)$ is a stationary flux, and we set this problem on the unit disk again for simplicity. As previously we will consider two types of boundary conditions, namely homogeneous Dirichlet and homogeneous Navier boundary conditions ([8]). By using the transformation $r = |x|$ and $\sigma(x) = \phi(|x|)$ the above partial differential equation (3) is converted into a fourth order ordinary differential equation which reads

$$\frac{1}{r} \left\{ r \left[\frac{1}{r} (r\phi')' \right]' \right\}' = \frac{1}{r} \phi' \phi'' + \lambda G(r) \quad (4)$$

where $' = \frac{d}{dr}$.

The Dirichlet boundary conditions that correspond to (4) are

$$\phi'(0) = 0, \quad \phi(1) = 0, \quad \phi'(1) = 0, \quad \lim_{r \rightarrow 0} r\phi'''(r) = 0, \quad (5)$$

the Navier boundary conditions of type one are

$$\phi'(0) = 0, \quad \phi(1) = 0, \quad \phi'(1) + \phi''(1) = 0, \quad \lim_{r \rightarrow 0} r\phi'''(r) = 0, \quad (6)$$

and the Navier boundary conditions of type two are

$$\phi'(0) = 0, \quad \phi(1) = 0, \quad \phi''(1) = 0, \quad \lim_{r \rightarrow 0} r\phi'''(r) = 0. \quad (7)$$

The condition $\phi'(0) = 0$ imposes the existence of an extremum at the origin. The conditions $\phi(1) = 0$ and $\phi'(1) = 0$ are the actual boundary conditions. For simplicity we take $G(r) = 1$, which physically means that the new material is being deposited uniformly on the unit disc. Using $\lim_{r \rightarrow 0} r\phi'''(r) = 0$ and integrating by parts, equation (4) gives

$$r \left[\frac{1}{r} (r\phi')' \right]' = \frac{1}{2} (\phi')^2 + \frac{1}{2} \lambda r^2. \quad (8)$$

Using the second transformation $w = r\phi'$, from equation (8) we get

$$r^2 w''(r) - rw'(r) = \frac{1}{2} w^2(r) + \frac{1}{2} \lambda r^4, \quad (9)$$

Corresponding to homogeneous Dirichlet boundary condition is

$$w'(0) = 0 \text{ and } w(1) = 0, \quad (10)$$

homogeneous Navier boundary condition of type one is

$$w'(0) = 0 \text{ and } w'(1) = 0, \quad (11)$$

and homogeneous Navier boundary condition of type two is

$$w'(0) = 0 \text{ and } w(1) = w'(1). \quad (12)$$

Equation (9) was numerically integrated by means of the use of a fourth order Runge-Kutta method in [7]. Now, we understand the solution of equation (9) belonging to the space $C^2[0, 1]$.

Equation (9) is a nonlinear, non self-adjoint and singular differential equation. Further more it has multiple solutions. Therefore discrete methods such as finite element method etc may not be applicable to pick all solutions together. These facts highlight the difficulties to deal with such an equation both analytically and numerically. Some recent theoretical progress has been built nevertheless regarding this type of boundary value problems as well some generalizations [2, 5, 6, 10, 12, 11]. The reader may appreciate in these references the wide range of mathematical techniques needed to analyze this sort of differential equations.

The aim of the present work is to find the numerically approximated solutions of the fourth order differential equation (4) with $G(r) \equiv 1$. To get the solutions of (4) we first compute the solutions of differential equation (9) using an iterative numerical scheme and compare our results to the ones in [7]. This numerical method became popularized in recent years under the name of variational iteration method (VIM) but it is in fact a reformulation of classical schemes (see [1, 21, 14, 15, 16, 19, 17, 22, 25, 18]). Recently, VIM are still under investigation, e.g., Wazwaz et al. ([26]) used it to find the approximate solution of nonlinear singular boundary value problem, Zhang et al. ([28]) applied it on a family of fifth-order convergent methods for solving nonlinear equations, Zellal et al. ([27]) used it on biological population model, Singh et al. ([24]) discussed it on a 2 point and 3 point nonlinear SBVPs.

The remainder of the paper has been organized as follows. In section 2, we describe the numerical method, show that it is well suited to approach the present boundary value problems, and illustrate how it works by solving explicitly a linearization of our nonlinear differential equation. In section 3, we use this method to solve numerically the non self-adjoint nonlinear singular boundary value problems under study and show a wide range of numerical results. In section 4 and 5, we place the numerical data. Finally, in section 6 we draw our main conclusions.

2 The numerical method

In order to explain the phenomenology of this method we consider a general non-linear differential equation of the form

$$Lw(r) + Nw(r) = f(r), \quad (13)$$

where L is the linear operator, N is the nonlinear operator and $f(r)$ is a known function. We can construct the correction functional to our iterative scheme applied to equation (13) as follows:

$$w_{n+1}(r) = w_n(r) + \int_0^r \mu(t) (Lw_n(t) + N\tilde{w}_n(t) - f(t)) dt, \quad (14)$$

where $\mu(t)$ is the Lagrange multiplier and \tilde{w}_n is of restricted variation i.e., $\delta\tilde{w}_n = 0$ ([23]). The Lagrange multiplier $\mu(t)$ can be identified optimally via the variational principle ([13]) and integration by parts. After getting the value of $\mu(t)$, we arrive at a recurrence relation defined by equation (14). We take a suitable initial approximation $w_0(r)$ in such a way such that this integral in equation (14) is convergent and hence we can compute $w_1(r)$, $w_2(r)$, \dots . The exact solution $w(r)$ of equation (13) can be found as

$$w(r) = \lim_{n \rightarrow \infty} w_n(r). \quad (15)$$

Before we solve equation (9) using (14) we shall discuss the properties of this method for the nonlinear singular boundary value problems associated to (9). From equation (14) and equation (9) we get the correction functional as

$$w_{n+1}(r) = w_n(r) + \int_0^r \mu(t) \left(t^2 w_n''(t) - t\tilde{w}_n'(t) - \frac{1}{2}\tilde{w}_n^2(t) - \frac{1}{2}\lambda t^4 \right) dt. \quad (16)$$

To find the value of $\mu(t)$ we take variations on both sides of (16) such that $\delta(t\tilde{w}_n'(t) + \frac{1}{2}\tilde{w}_n^2(t)) = 0$. Eq (16) becomes

$$\delta w_{n+1}(r) = \delta w_n(r) + \delta \int_0^r \mu(t) \left(t^2 w_n''(t) - t\tilde{w}_n'(t) - \frac{1}{2}\tilde{w}_n^2(t) - \frac{1}{2}\lambda t^4 \right) dt, \quad (17)$$

or equivalently,

$$\delta w_{n+1}(r) = \delta w_n(r) + \delta \int_0^r \mu(t) t^2 w_n''(t) dt. \quad (18)$$

By using integration by parts we get

$$\delta w_{n+1}(r) = (1 - \mu'(r)r^2 - 2r\mu(r)) \delta w_n(r) + \mu(r)r^2 \delta w_n'(r) + \int_0^r (\mu''(t)t^2 + 4t\mu'(t) + 2\mu(t)) \delta w_n dt. \quad (19)$$

The extremum condition imposed on w_{n+1} gives $\delta w_{n+1} = 0$ ([23]), and from (19) we arrive at the following stationary conditions

$$1 - \mu'(r)r^2 - 2r\mu(r) = 0, \quad (20)$$

$$\mu(r) = 0, \quad (21)$$

$$\mu''(t)t^2 + 4t\mu'(t) + 2\mu(t) = 0. \quad (22)$$

By solving (20-22), we get the optimal value of $\mu(t)$, given by

$$\mu(t) = \frac{t-r}{t^2}. \quad (23)$$

Hence the correction functional (16) becomes

$$w_{n+1}(r) = w_n(r) + \int_0^r \frac{t-r}{t^2} \left(t^2 w_n''(t) - t w_n'(t) - \frac{1}{2} w_n^2(t) - \frac{1}{2} \lambda t^4 \right) dt. \quad (24)$$

Equation (24) gives rise to a sequence $\{w_n(r)\}$. If this sequence $\{w_n(r)\}$ is convergent then its limit gives the exact solution of the nonlinear singular differential equation (9). Now we shall prove that this sequence $\{w_n(r)\}$ is well defined. This fact is established by means of the following Lemma.

Lemma 2.1. *Let $w_n(r)$, $n = 0, 1, 2, \dots$, satisfy the following properties:*

- P_1 : $w_n'(0) = 0$,
- P_2 : $\lim_{r \rightarrow 0^+} w_n(r) = 0$,
- P_3 : $w_n''(r) \in C^2([0, 1])$.

Then $\frac{w_n(r)}{r^2}$ and $\frac{w_n'(r)}{r}$ are bounded on $[0, 1]$ for all $n \in \mathbb{N}_0$.

Proof. We have $\lim_{r \rightarrow 0^+} \frac{w_0(r)}{r^2} = \lim_{r \rightarrow 0^+} \frac{w_0'(r)}{2r} = \lim_{r \rightarrow 0^+} \frac{w_0''(r)}{2}$. But $w_0''(r)$ is bounded on $[0, 1]$. So we conclude that $\frac{w_0(r)}{r^2}$ is bounded on $[0, 1]$. By a similar argument, since P_1 , P_2 , and P_3 hold true for all $n \in \mathbb{N}$, $\frac{w_n(r)}{r^2}$ is bounded on $[0, 1]$ for all $n \in \mathbb{N}$. The boundedness of $\frac{w_n'(r)}{r}$ follows from the same argument. \square

Lemma 2.2. *Let $w_0(r)$ be the initial approximation of (24) such that*

$$w_0'(0) = 0, \quad \lim_{r \rightarrow 0^+} w_0(r) = 0 \quad \text{and} \quad w_0''(r) \in C^2([0, 1]). \quad (25)$$

Let $w_n(r)$, $n = 1, 2, \dots$, be defined by (24). Then $w_n(r)$, $n = 1, 2, \dots$, satisfies the following properties:

- P_1 : $w_n'(0) = 0$,
- P_2 : $\lim_{r \rightarrow 0^+} w_n(r) = 0$,
- P_3 : $w_n''(r) \in C^2([0, 1])$.

Proof. We proof the statement by induction. For $n = 0$ properties P_1 , P_2 , and P_3 are true. Now we prove that P_1 , P_2 , and P_3 are true for $n = 1$. From equation (24) by setting $n = 0$ we get

$$w_1(r) = w_0(r) + \int_0^r \frac{t-r}{t^2} \left(t^2 w_0''(t) - t w_0'(t) - \frac{1}{2} w_0^2(t) - \frac{1}{2} \lambda t^4 \right) dt. \quad (26)$$

By differentiating both sides of equation (26) with respect to r we get

$$\begin{aligned} w_1'(r) &= w_0'(r) + \frac{r-r}{r^2} \left(r^2 w_0''(r) - r w_0'(r) - \frac{1}{2} w_0^2(r) - \frac{1}{2} \lambda r^4 \right) \frac{d}{dr}(r) \\ &\quad - \lim_{t \rightarrow 0^+} \left(\frac{t-r}{t^2} \left(t^2 w_0''(t) - t w_0'(t) - \frac{1}{2} w_0^2(t) - \frac{1}{2} \lambda t^4 \right) \right) \frac{d}{dr}(0) \\ &\quad + \int_0^r \frac{-1}{t^2} \left(t^2 w_0''(t) - t w_0'(t) - \frac{1}{2} w_0^2(t) - \frac{1}{2} \lambda t^4 \right) dt. \end{aligned} \quad (27)$$

Using (25) we can easily get that

$$w_1'(r) = w_0'(r) + \int_0^r \frac{-1}{t^2} \left(t^2 w_0''(t) - t w_0'(t) - \frac{1}{2} w_0^2(t) - \frac{1}{2} \lambda t^4 \right) dt \quad (28)$$

and

$$w_1''(r) = w_0''(r) - \frac{1}{r^2} \left(r^2 w_0''(r) - r w_0'(r) - \frac{1}{2} w_0^2(r) - \frac{1}{2} \lambda r^4 \right). \quad (29)$$

By setting $r = 0$ in equation (28) we get $w_1'(0) = w_0'(0) = 0$ via the application of Lemma 2.1.

Using equation (25) and Lemma 2.1 it can be easily concluded that the integrand in the integral of (26) is bounded on $[0, 1]$. Taking $\lim_{r \rightarrow 0^+}$ on both sides of equation (26), we get $\lim_{r \rightarrow 0^+} w_1(r) = \lim_{r \rightarrow 0^+} w_0(r) + 0 = 0$.

Now from equation (29), we get

$$|w_1''(r)| \leq |w_0''(r)| + \left| \frac{1}{r^2} \left(r^2 w_0''(r) - r w_0'(r) - \frac{1}{2} w_0^2(r) - \frac{1}{2} \lambda r^4 \right) \right|. \quad (30)$$

A simple application of (25) and Lemma 2.1 on the second term of the right hand side of equation (30) reveals that it is bounded on $[0, 1]$. Thus $w_1''(r)$ is bounded on $[0, 1]$. Moreover $w_1''(r)$ is continuous with the obvious definition of $w_1''(0)$, as can be immediately checked from equation (29) and an argument akin to the one in the proof of Lemma 2.1.

Therefore P_1 , P_2 , and P_3 hold for $n = 1$.

Let us now assume that P_1 , P_2 , and P_3 hold for an arbitrary n , that is

$$w_n'(0) = 0, \quad \lim_{r \rightarrow 0^+} w_n(r) = 0 \quad \text{and} \quad w_n''(r) \quad (31)$$

is bounded and continuous on $[0, 1]$.

Now we will show that P_1 , P_2 , and P_3 hold for $n + 1$ too. From equation (24) we get

$$w_{n+1}(r) = w_n(r) + \int_0^r \frac{t-r}{t^2} \left(t^2 w_n''(t) - t w_n'(t) - \frac{1}{2} w_n^2(t) - \frac{1}{2} \lambda t^4 \right) dt. \quad (32)$$

Differentiating both sides with respect to r , we get

$$w_{n+1}'(r) = w_n'(r) + \int_0^r \frac{-1}{t^2} \left(t^2 w_n''(t) - t w_n'(t) - \frac{1}{2} w_n^2(t) - \frac{1}{2} \lambda t^4 \right) dt, \quad (33)$$

and

$$w''_{n+1}(r) = w''_n(r) - \frac{1}{r^2} \left(r^2 w''_n(r) - r w'_n(r) - \frac{1}{2} w_n^2(r) - \frac{1}{2} \lambda r^4 \right). \quad (34)$$

By setting $r = 0$ in equation (33) we get $w'_{n+1}(0) = w'_n(0) = 0$ by Lemma 2.1.

Using equation (31) and Lemma 2.1 it is easy to see that the integrand inside the integral of (32) is bounded on $[0, 1]$. Taking $\lim_{r \rightarrow 0^+}$ on both sides of equation (32) we get $\lim_{r \rightarrow 0^+} w_{n+1}(r) = \lim_{r \rightarrow 0^+} w_n(r) + 0 = 0$.

Now from equation (34) we get

$$|w''_{n+1}(r)| \leq |w''_n(r)| + \left| \frac{1}{r^2} \left(r^2 w''_n(r) - r w'_n(r) - \frac{1}{2} w_n^2(r) - \frac{1}{2} \lambda r^4 \right) \right|. \quad (35)$$

A simple application of (31) and Lemma 2.1 on the second term of the right hand side of equation (35) shows that it is bounded on $[0, 1]$. Thus $w''_{n+1}(r)$ is bounded on $[0, 1]$ as well. Furthermore $w''_n(r)$ is continuous with the evident definition of $w''_n(0)$, as can be seen from equation (34) and an analogous argument to that in the proof of Lemma 2.1.

Thus P_1 , P_2 , and P_3 hold true for $n + 1$.

By mathematical induction we conclude that P_1 , P_2 , and P_3 hold true for all $n \in \mathbb{N}$. \square

Lemmata 2.1 and 2.2 show that the iterations in our numerical method lead to a well-defined procedure; now we will illustrate how the method works with a particular example. If $\lambda = 0$ then $w(r) \equiv 0$ is obviously a solution. And if $|\lambda|$ is very small then the nonlinearity in equation (9) is $O(\lambda^2)$ and therefore negligible. In this limit the equation to be solved is

$$r^2 w''(r) - r w'(r) = \frac{1}{2} \lambda r^4. \quad (36)$$

This is a linear differential equation of Euler type and therefore explicitly solvable, but instead using standard techniques we will proceed to solve it using our numerical method. A homogeneity argument suggests using an arbitrary fourth degree polynomial as initial condition for the iterations, that is

$$w_0(r) = a_4 r^4 + a_3 r^3 + a_2 r^2 + a_1 r + a_0,$$

where $a_4, a_3, a_2, a_1, a_0 \in \mathbb{R}$. The first iteration shows that the only way to maintain this procedure finite is to set $a_1 = 0$, so we will do so from now on. Now it is easy to compute the n^{th} iteration to find

$$w_n(r) = \left(\frac{a_4}{3^n} + \frac{\lambda}{16} - \frac{\lambda}{16 \times 3^n} \right) r^4 + \frac{a_3}{2^n} r^3 + a_2 r^2 + a_0.$$

Also, it is immediate to check that the limit

$$w_\infty(r) := \lim_{n \rightarrow \infty} w_n(r) = \frac{\lambda}{16} r^4 + a_2 r^2 + a_0$$

solves the equation (36) for any $a_2, a_0 \in \mathbb{R}$. These parameters are fixed by the boundary conditions, in particular, the condition $\phi'(0) = 0$, common to both boundary value problems, translates to

$$\lim_{r \rightarrow 0^+} \frac{w(r)}{r} = 0 \implies a_0 = 0.$$

Finally, for the Dirichlet problem $w(1) = 0$ and we find

$$w_D(r) = \frac{\lambda}{16} r^2 (r^2 - 1),$$

for the Navier problem of type one $w'(1) = 0$ and we get

$$w_{N_1}(r) = \frac{\lambda}{16} r^2 (r^2 - 2),$$

and for the Navier problem of type two $w(1) = w'(1)$ and we get

$$w_{N_2}(r) = \frac{\lambda}{16} r^2 (r^2 - 3).$$

These results together with the common boundary condition $\phi(1) = 0$ yield the linear approximations

$$\begin{aligned} \phi_D(r) &= \frac{\lambda}{64} (r^2 - 1)^2, \\ \phi_{N_1}(r) &= \frac{\lambda}{64} (r^4 - 4r^2 + 3), \\ \phi_{N_2}(r) &= \frac{\lambda}{64} (r^4 - 6r^2 + 5), \end{aligned}$$

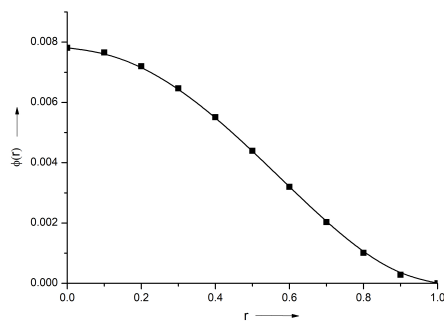
to the solutions of equation (4) with $G(r) \equiv 1$, i. e. solutions to the linear equation

$$\frac{1}{r} \left\{ r \left[\frac{1}{r} (r\phi')' \right]' \right\}' = \lambda,$$

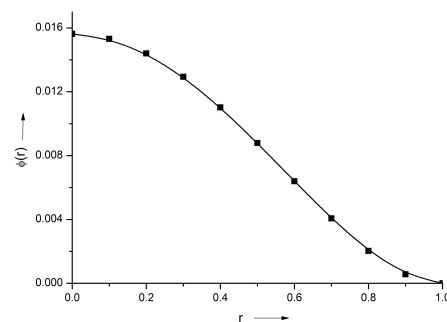
for the respective sets of boundary conditions. These linear approximations are represented in Figure 2.1.

A qualitative agreement can be appreciated between the linear approximations and the actual solutions to the nonlinear problems numerically computed in the next section. Of course, multiplicity of solutions is not found in the linear regime, this phenomenon only appears when the full nonlinear problem is considered, see section 3. In this respect, these linear approximations approximate the solutions of the nonlinear problem that lie in vicinity of the origin, the so called lower solutions in the next section. One can appreciate the common geometric features shared by nonlinear lower solutions and linear approximations. Another phenomenon that does not appear at the linear approximation level is non-existence of solutions: this takes place for values of λ that lie beyond the range of validity of this approximation. Both phenomena of multiplicity and non-existence of solutions to the nonlinear boundary value problems are discussed in detail in the following section.

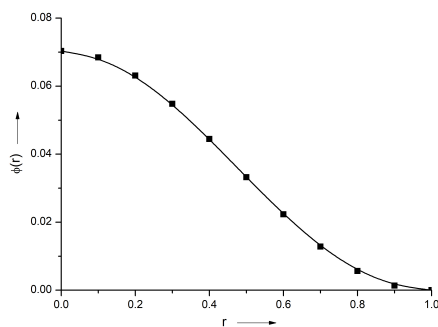
All of these considerations show how our numerical method works, and we will now use it to numerically solve the nonlinear problems under study in the next section.



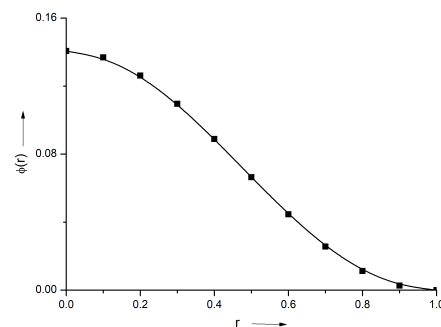
(a) $\lambda = 1/2$



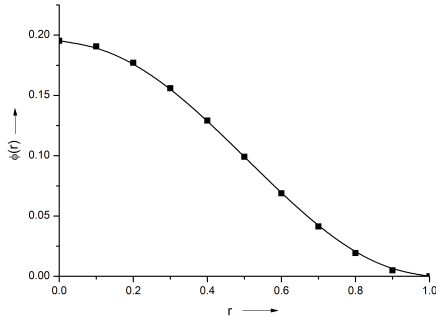
(b) $\lambda = 1$



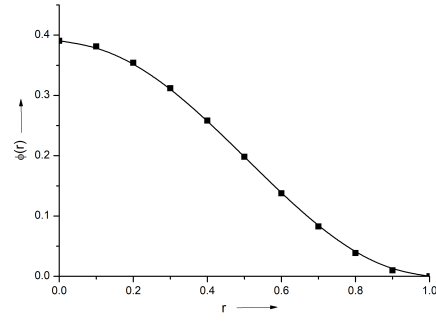
(c) $\lambda = 1/2$



(d) $\lambda = 1$



(e) $\lambda = 1/2$



(f) $\lambda = 1$

Figure 2.1: Linear approximations to the solutions of equation (4) with $G(r) \equiv 1$ for Dirichlet boundary conditions with $\lambda = 1/2$ (figure (a)) and $\lambda = 1$ (figure (b)), and for Navier boundary conditions of type one with $\lambda = 1/2$ (figure (c)) $\lambda = 1$ (figure (d)), and for Navier boundary conditions of type two with $\lambda = 1/2$ (figure (e)) and $\lambda = 1$ (figure (f)), as explained in the text. Of course, only the solution in the vicinity of the origin is approximated.

3 Numerical illustrations

In this section we will discuss about the solvability of differential equation (4) associated to either homogeneous Dirichlet boundary conditions or homogeneous Navier boundary conditions of both types. For this purpose we first apply our iterative numerical scheme on equation (9) and after that using the transformation $w(r) = r\phi'(r)$ and the left boundary conditions we get the solution of (4). In [8], they arrive at two cases:

Case (a): $\lambda \geq 0$.

They observe that for $\lambda = 0$ there are two solutions. One is trivial and the other is non trivial. For $0 < \lambda < \lambda_{\text{critical}}$ they always get two non-trivial solutions. Since the solutions are ordered, they call them respectively the upper and lower solution. The critical value of λ , i.e. $\lambda_{\text{critical}}$, is approximated to be 11.34 and 169 corresponding to Navier boundary condition of type two and Dirichlet boundary condition ([8]) respectively. For $\lambda > \lambda_{\text{critical}}$ there does not exist any numerical solutions. No conclusion is given for Navier boundary condition of type one.

Case (b): $\lambda < 0$.

No conclusion is given for both types of boundary conditions.

3.1 Navier boundary condition of type one

Here we consider equation (9) subject to

$$w'(0) = 0 \text{ and } w'(1) = 0. \quad (37)$$

Let $w_0(r) = ar^2$, $a \in \mathbb{R}$, be an initial approximation. This choice satisfies all the assumptions of Lemma 2.2. By setting $n = 0$ in equation (24) we get

$$w_1(r) = w_0(r) + \int_0^r \frac{t-r}{t^2} \left(t^2 w_0''(t) - t w_0'(t) - \frac{1}{2} w_0^2(t) - \frac{1}{2} \lambda t^4 \right) dt. \quad (38)$$

Successively we get

$$w_1(r) = \frac{a^2 r^4}{24} + ar^2 + \frac{\lambda r^4}{24}, \quad (39)$$

$$w_2(r) = \frac{a^4 r^8}{64512} + \frac{a^3 r^6}{720} + \frac{a^2 \lambda r^8}{32256} + \frac{a^2 r^4}{18} + \frac{1}{720} a \lambda r^6 + ar^2 + \frac{\lambda^2 r^8}{64512} + \frac{\lambda r^4}{18}, \quad (40)$$

and so on.

By using Mathematica we have computed w_n for $n = 3, 4, 5, 6, 7$, but due to lack of space we could not list all of them. To calculate $\phi(r)$, here we take $w(r) = w_7(r)$ as an approximate solution of (9). So, we found $w(r)$ is a function of r including a as a constant and λ as a parameter. By using the boundary condition $w'(1) = 0$ we have computed the values of a corresponding to each λ . Now from transformation $w(r) = r\phi'(r)$ and boundary condition $\phi(1) = 0$ we have computed the solution $\phi(r)$ corresponding to different values of λ . We arrive at two cases depending on λ .

Case (c): $\lambda \geq 0$.

Here, We observe the same remarks as in Case (a). The critical value of λ , i.e. $\lambda_{\text{critical}}$, is approximately 31.94.

For $\lambda > \lambda_{\text{critical}}$ numerical solutions do not exist as the values of a become imaginary. In table 1 and table 2 we tabulate residual errors. We have also plotted the graphs of $\phi(r)$. We see that the solutions are moving towards each other as λ is increased [see Figure 5.1].

Case (d): $\lambda < 0$.

We observe that we always get two numerical solutions corresponding to each negative λ . One solution is positive (namely the positive solution) and the other solution is negative (namely the negative solution). There is no negative critical λ . We list residue errors in tables 3 and 4. We see that the solutions are aparting from each other as λ is decreased [see Figure 5.2].

3.2 Navier boundary condition of type two

In this subsection, we consider :

$$w'(0) = 0 \text{ and } w(1) = w'(1) \quad (41)$$

corresponding to equation (9).

Here we also have the same iterations as in (39) and (40). To calculate $\phi(r)$, here we take $w(r) = w_7(r)$ as an approximate solution of (9). By using the boundary condition $w(1) = w'(1)$, $w(r) = r\phi'(r)$ and boundary condition $\phi(1) = 0$, we have computed the solution $\phi(r)$ corresponding to different values of λ . We arrive at two cases depending on λ .

Case (e): $\lambda \geq 0$.

Same remarks are made as in Case (c) to the subsection 3.1. The critical value of λ , i.e. $\lambda_{\text{critical}}$, is approximately 11.34 ([8]). In table 5 and table 6 we tabulate residual errors, and in figure 5.3 we place the approximate solutions graph.

Case (f): $\lambda < 0$.

All remarks are same to Case (d) in subsection 3.1. In table 7, table 8 and figure 5.4 we place the numerical data of approximate solutions.

3.3 Dirichlet boundary condition

Furthermore, here we consider Dirichlet boundary conditions

$$w'(0) = 0 \text{ and } w(1) = 0. \quad (42)$$

The iteration scheme is given by equation (24).

Here we also consider $w_0(r) = ar^2$, $a \in \mathbb{R}$, as an initial approximation. Then we compute $w_1, w_2, w_3, w_4, w_5, w_6$. We take $w_6(r)$ as approximate solution. To calculate the values of a we use the boundary condition $w(1) = 0$. Then using the transformation $w(r) = r\phi'$ and $\phi(1) = 0$ we easily get the approximate solution $\phi(r)$. Here we also arrive at two different cases depending on the value of parameter λ .

Case (g): $\lambda \geq 0$.

Here we have also noticed analogous remarks as in subsection 3.1. The critical value of λ , i.e. $\lambda_{\text{critical}}$, is approximately 169 ([8]). The properties of the solutions are presented in table 9 to table 10. We have displayed few graphs [Figure 5.5] corresponding to some positive values of λ .

Case (h): $\lambda < 0$.

Again, we observe same remarks as in subsection 3.1. In table 11, table 12 and figure 5.6 we list all the numerical data of approximate solutions.

4 Tables

Here, we have listed bellow some numerical data of approximate solutions corresponding to section 3.

4.1 Navier boundary condition of type one

Table 1: Upper solution residue errors for Navier boundary conditions of type one:

r	$\lambda = 0$	$\lambda = 15$	$\lambda = 20$	$\lambda = 31$
0	0	0	0	0
0.1	-0.000155912	-0.000114429	-9.98657E-05	-5.76457E-05
0.2	-0.000343263	-0.000371915	-0.000365384	-0.000290267
0.3	0.001588386	0.000620694	0.000333768	-0.000267199
0.4	0.006171169	0.003943101	0.003114494	0.000803931
0.5	0.008731215	0.007584368	0.006742658	0.003148673
0.6	0.003260515	0.00721201	0.007721714	0.005805328
0.7	-0.010610475	0.000189979	0.003211949	0.007033732
0.8	-0.026235626	-0.011575058	-0.006229739	0.00548626
0.9	-0.035139344	-0.02270068	-0.01667245	0.001231356

Table 2: Lower solution residue errors for Navier boundary conditions of type one:

r	$\lambda = 0$	$\lambda = 15$	$\lambda = 20$	$\lambda = 31$
0	0	0	0	0
0.1	0	-8.87083E-06	-1.3327E-05	-3.45209E-05
0.2	0	-6.53946E-05	-9.45309E-05	-0.000206661
0.3	0	-0.00019217	-0.000258526	-0.000380835
0.4	0	-0.000373617	-0.000445102	-0.00015177
0.5	0	-0.00056198	-0.000542526	0.000847379
0.6	0	-0.000702365	-0.000448957	0.00257569
0.7	0	-0.000770031	-0.000146034	0.004456882
0.8	0	-0.00081014	0.000244377	0.005612047
0.9	0	-0.00097216	0.000437111	0.005313773

Table 3: Positive solution residue errors for Navier boundary conditions of type one:

r	$\lambda = -1$	$\lambda = -40$	$\lambda = -60$	$\lambda = -100$
0	0	0	0	0
0.1	-0.000158668	-0.000275753	-0.000348062	-0.000530218
0.2	-0.000339023	8.87605E-05	0.000591477	0.002846296
0.3	0.001659012	0.005084608	0.007385895	0.012677871
0.4	0.006308302	0.010250819	0.010473629	0.001611918
0.5	0.00874322	0.002958666	-0.005421612	-0.0359395
0.6	0.00289219	-0.018916565	-0.033821897	-0.059343222
0.7	-0.011384538	-0.040769892	-0.05065471	-0.040737203
0.8	-0.027110199	-0.046053985	-0.040944067	0.006597174
0.9	-0.035680636	-0.03035376	-0.009364712	0.056747965

Table 4: Negative solution residue errors for Navier boundary conditions of type one:

r	$\lambda = -1$	$\lambda = -40$	$\lambda = -60$	$\lambda = -100$
0	0	0	0	0
0.1	4.50911E-07	1.20523E-05	1.55973E-05	2.05055E-05
0.2	3.62314E-06	0.000109664	0.000148369	0.000209255
0.3	1.23135E-05	0.000447296	0.00064218	0.000990024
0.4	2.94528E-05	0.001327808	0.002032183	0.003435276
0.5	5.81282E-05	0.003293586	0.005368521	0.009921185
0.6	0.000101552	0.007206178	0.012468993	0.025072982
0.7	0.000162956	0.014243773	0.026048476	0.056683522
0.8	0.000245387	0.025666456	0.049332478	0.115399675
0.9	0.000351386	0.042091333	0.08437909	0.210205598

4.2 Navier boundary condition of type two

Table 5: Upper solution residue errors for Navier boundary conditions of type two:

r	$\lambda = 0$	$\lambda = 8$	$\lambda = 10$	$\lambda = 11.34$
0	0	0	0	0
0.1	-3.59128E-05	-2.41406E-05	-1.98602E-05	-1.36854E-05
0.2	-0.00019189	-0.000144885	-0.000124646	-9.1929E-05
0.3	-0.000229253	-0.00026456	-0.000257591	-0.000223497
0.4	0.000379522	-7.65776E-05	-0.000194005	-0.000294198
0.5	0.001951425	0.00073382	0.000336884	-0.000128778
0.6	0.004095042	0.002209409	0.001454893	0.000417341
0.7	0.005675344	0.003964315	0.002983797	0.001363933
0.8	0.005331432	0.005273065	0.004455361	0.00255888
0.9	0.002218034	0.005369172	0.005271528	0.003704074

Table 6: Lower solution residue errors for Navier boundary conditions of type two:

r	$\lambda = 0$	$\lambda = 8$	$\lambda = 10$	$\lambda = 11.34$
0	0	0	0	0
0.1	0	-5.31802E-06	-8.03463E-06	-1.31725E-05
0.2	0	-3.95382E-05	-5.77125E-05	-8.90043E-05
0.3	0	-0.00011771	-0.000161094	-0.000219188
0.4	0	-0.000232269	-0.00028476	-0.000297926
0.5	0	-0.000352779	-0.00035549	-0.000159086
0.6	0	-0.000434856	-0.00028637	0.000339477
0.7	0	-0.000436068	-1.38768E-05	0.001227054
0.8	0	-0.00033461	0.000467775	0.002372209
0.9	0	-0.000146031	0.001087285	0.003501342

Table 7: Positive solution residue errors for Navier boundary conditions of type two:

r	$\lambda = -1$	$\lambda = -50$	$\lambda = -100$	$\lambda = -160$
0	0	0	0	0
0.1	-3.71856E-05	-9.52198E-05	-0.000171484	-0.0003356
0.2	-0.000196294	-0.000293491	-0.000196499	0.000690227
0.3	-0.000221431	0.000634465	0.002515105	0.007458185
0.4	0.000437305	0.003624522	0.007340292	0.009598758
0.5	0.002086313	0.006721547	0.006882551	-0.008688033
0.6	0.004270952	0.005539989	-0.00553502	-0.039604188
0.7	0.005768587	-0.002998379	-0.026584976	-0.055617692
0.8	0.005166738	-0.017397284	-0.043629852	-0.037115791
0.9	0.001651162	-0.031769072	-0.043368929	0.015496504

Table 8: Negative solution residue errors for Navier boundary conditions of type two:

r	$\lambda = -1$	$\lambda = -50$	$\lambda = -100$	$\lambda = -160$
0	0	0	0	0
0.1	0	1.0114E-05	1.37015E-05	1.59205E-05
0.2	0	9.66798E-05	0.000143445	0.000179917
0.3	1.21638E-05	0.000422316	0.000702496	0.000963885
0.4	2.92389E-05	0.001356286	0.002538349	0.003806251
0.5	5.80708E-05	0.003662489	0.007683917	0.012541867
0.6	0.000102229	0.008777896	0.020536832	0.036345698
0.7	0.000165517	0.019165906	0.049731562	0.095077006
0.8	0.000251823	0.038627935	0.110500915	0.227275426
0.9	0.000364852	0.072242013	0.226171011	0.497848871

4.3 Dirichlet boundary condition

Table 9: Lower solution residue errors for Dirichlet boundary conditions:

r	$\lambda = 0$	$\lambda = 100$	$\lambda = 150$	$\lambda = 168.5$
0	0	0	0	0
0.1	0	-0.000206385	-0.000456193	-0.000792126
0.2	0	-0.001202861	-0.00172148	-0.001148293
0.3	0	-0.002150566	0.000877891	0.009654358
0.4	0	-0.001088836	0.011254878	0.028840292
0.5	0	0.002659014	0.023546219	0.03096701
0.6	0	0.00643131	0.025416409	0.002113967
0.7	0	0.00420898	0.011384789	-0.032940028
0.8	0	-0.012205803	-0.008754913	-0.02467811
0.9	0	-0.053923736	-0.012406316	0.083542791

Table 10: Upper solution residue errors for Dirichlet boundary conditions:

r	$\lambda = 0$	$\lambda = 100$	$\lambda = 150$	$\lambda = 168.5$
0	0	0	0	0
0.1	-0.002203063	-0.001886917	-0.001342885	-0.000877685
0.2	0.033797318	0.011517037	0.002749495	-0.000788042
0.3	0.030922362	0.044532539	0.02827772	0.012361223
0.4	-0.014345268	-0.003159996	0.035900291	0.03213499
0.5	-0.022139308	-0.012445316	-0.020163177	0.027844336
0.6	-0.060894281	-0.165508967	-0.095517516	-0.01052225
0.7	0.016518058	-0.068424986	-0.010280418	-0.047258847
0.8	0.076289167	0.097795772	-0.004867326	-0.026755307
0.9	0.756076643	0.455082275	0.218123002	0.107541122

Table 11: Negative solution residue errors for Dirichlet boundary conditions:

r	$\lambda = -1$	$\lambda = -10$	$\lambda = -15$	$\lambda = -25$
0	0	0	0	0
0.1	1.37E-06	1.32986E-05	1.96493E-05	3.18005E-05
0.2	1.09624E-05	0.000108594	0.00016204	0.000267254
0.3	3.71163E-05	0.000377932	0.00057214	0.000969753
0.4	8.8313E-05	0.000928682	0.001429442	0.002498697
0.5	0.000173129	0.001878535	0.002937946	0.005288295
0.6	0.000300006	0.003333426	0.005277309	0.009716634
0.7	0.000476799	0.005340493	0.008494767	0.015794103
0.8	0.000710047	0.00780818	0.012317241	0.022597391
0.9	0.0010039	0.010388382	0.015872278	0.027416471

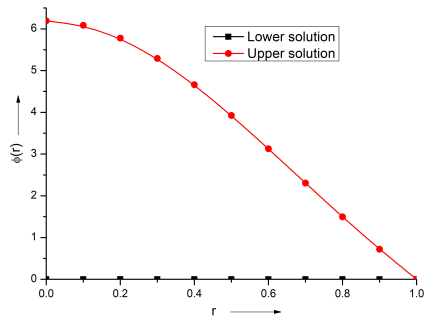
Table 12: Positive solution residue errors for Dirichlet boundary conditions:

r	$\lambda = -1$	$\lambda = -10$	$\lambda = -15$	$\lambda = -25$
0	0	0	0	0
0.1	-0.002200389	-0.002169851	-0.002147706	-0.00209184
0.2	0.034043159	0.036262321	0.03749797	0.039966042
0.3	0.030454157	0.025927616	0.023170528	0.017144747
0.4	-0.144959813	-0.158409209	-0.165767258	-0.18015219
0.5	-0.022137696	-0.02202973	-0.021897521	-0.02148112
0.6	-0.058843725	-0.039859043	-0.028938252	-0.006427889
0.7	0.016822394	0.019683635	0.021384849	0.025094771
0.8	0.078154323	0.097632679	0.11090339	0.144151755
0.9	0.802566715	0.109459893	0.130400343	0.186695393

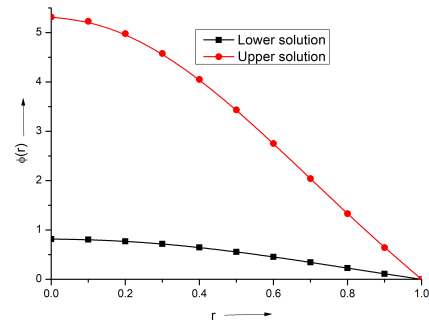
5 Figures

Here we have placed below approximate solutions graph corresponding to different types of boundary condition.

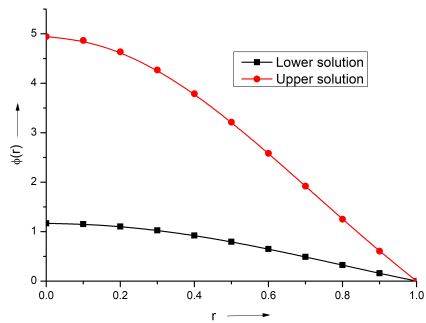
5.1 Navier boundary condition of type one



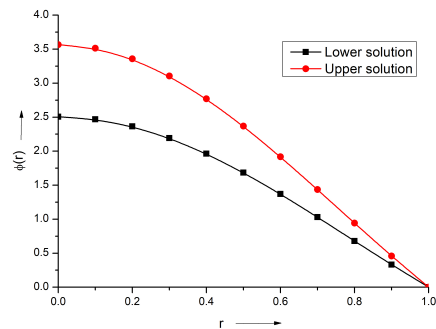
(a) $\lambda = 0$



(b) $\lambda = 15$

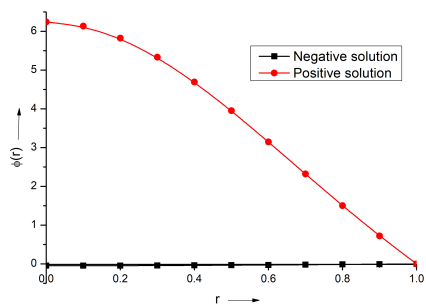


(c) $\lambda = 20$

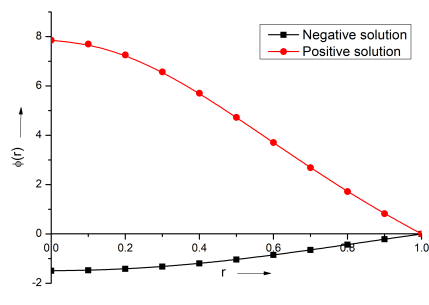


(d) $\lambda = 31$

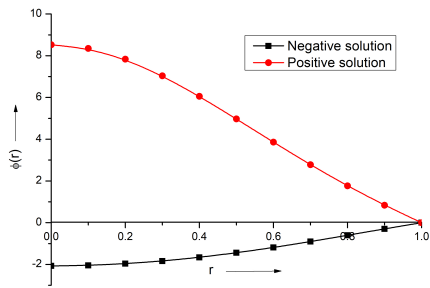
Figure 5.1: Graph of $\phi(r)$ versus r for positive λ .



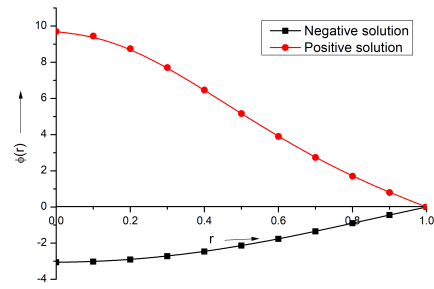
(a) $\lambda = -1$



(b) $\lambda = -40$



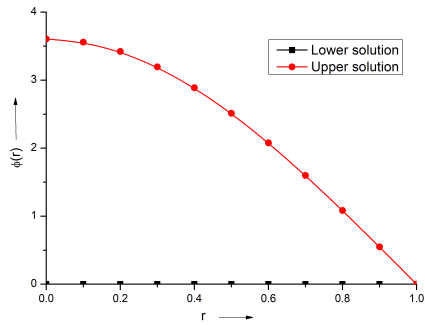
(c) $\lambda = -60$



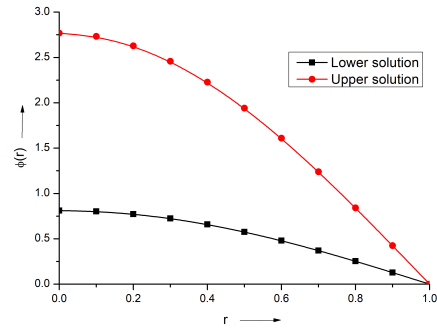
(d) $\lambda = -100$

Figure 5.2: Graph of $\phi(r)$ versus r for negative λ .

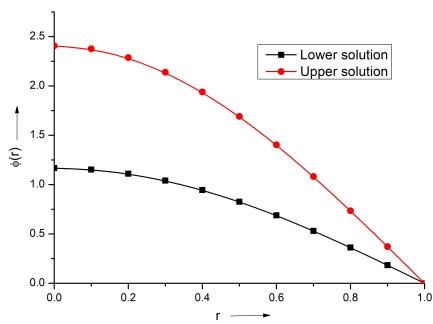
5.2 Navier boundary condition of type two



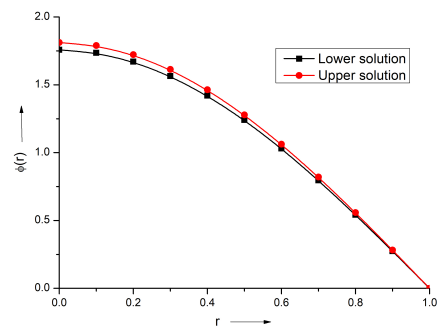
(a) $\lambda = 0$



(b) $\lambda = 8$

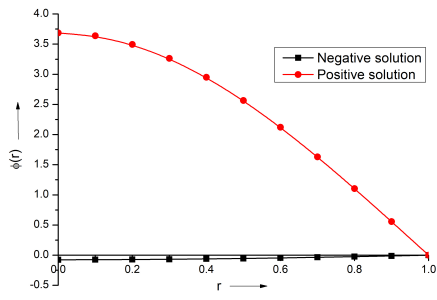


(c) $\lambda = 10$

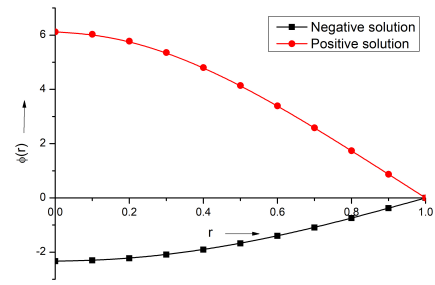


(d) $\lambda = 11.34$

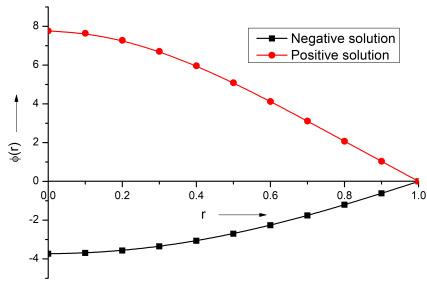
Figure 5.3: Graph of $\phi(r)$ versus r for positive λ .



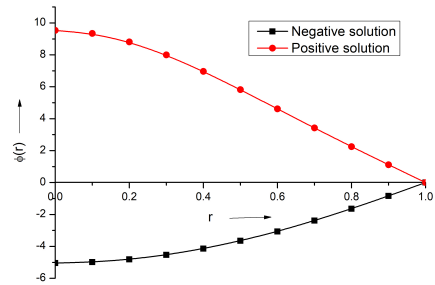
(a) $\lambda = -1$



(b) $\lambda = -50$



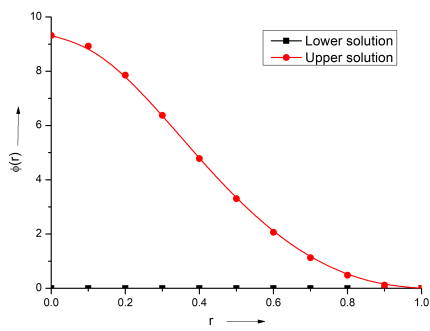
(c) $\lambda = -100$



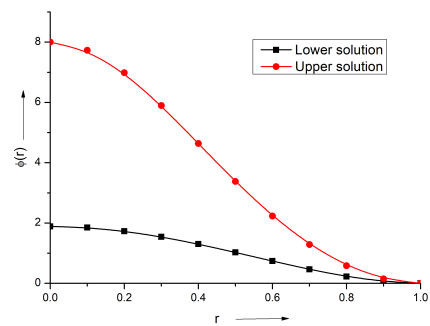
(d) $\lambda = -160$

Figure 5.4: Graph of $\phi(r)$ versus r for negative λ .

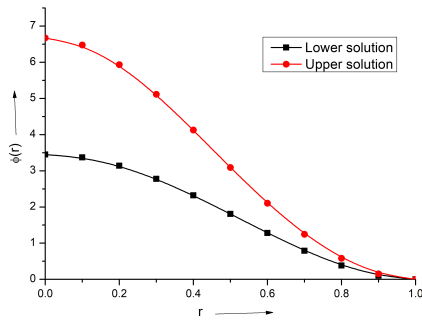
5.3 Dirichlet boundary condition



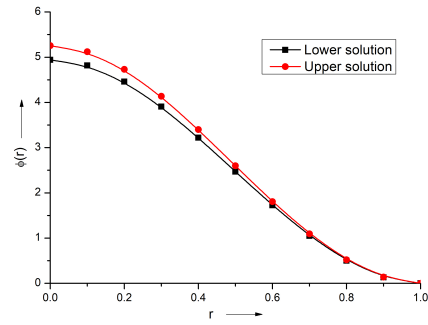
(a) $\lambda = 0$



(b) $\lambda = 100$

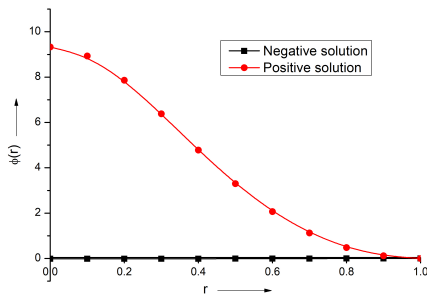


(c) $\lambda = 150$

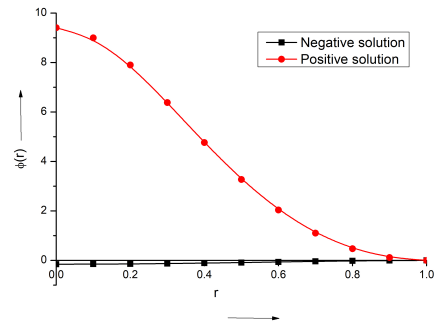


(d) $\lambda = 168.5$

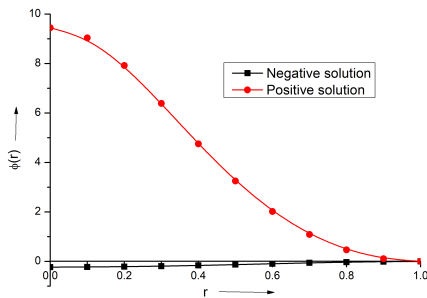
Figure 5.5: Graph of $\phi(r)$ versus r for positive λ .



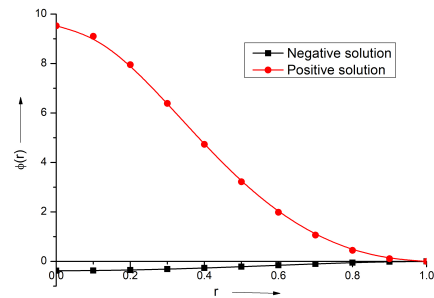
(a) $\lambda = -1$



(b) $\lambda = -10$



(c) $\lambda = -15$



(d) $\lambda = -25$

Figure 5.6: Graph of $\phi(r)$ versus r for negative λ .

6 Conclusions

In this paper, we have applied an iterative numerical method to nonlinear singular boundary value problems that arise in the theory of epitaxial growth. The proposed technique gives us approximate numerical solutions that are very close to exact solutions of the given differential equation. We have shown that for negative values of the forcing parameter λ two solutions always coexist: they are ordered and one is negative and the other positive. For more negative values of this parameter the solutions separate. When the value of this parameter is set to zero then one of the solutions becomes trivial but there still exists a second, nontrivial and positive, solution.

For positive values of λ below some critical threshold, which we have numerically estimated, there exist two ordered solutions, both nontrivial and positive, which become closer as the value of λ increases. We conjecture that both solutions merge into a single solution (still nontrivial and positive) when λ is set to its critical value. No solutions were numerically detected for supercritical values of λ . The results for the three different sets of boundary conditions we have considered herein show a qualitative agreement, although they do not behave in the same quantitative way. Also note that the present results agree with and extend those in [7], which were obtained by means of a fourth order Runge-Kutta method.

We expect the present results to have an impact in the understanding of these theoretical models of epitaxial growth. As we have seen the properties of the solution set depend on the value of the parameter λ . This parameter has a clear physical meaning: it is the rate at which new material is deposited onto the epitaxially growing solid. The fact that we take $G(r) \equiv 1$ in equation (4) means that this rate is homogeneous. Our numerical analysis shows that two stationary solutions exist if λ is small enough. The lower solution, if the full time dependent model were considered, should be dynamically stable, while the upper solution should be unstable. This means that, if the deposition rate is small enough, one should observe, instead of the system growing, the formation of a stationary mound, at least for suitable initial conditions. The formation of this stationary mound, which may look like a counterintuitive phenomenon in the presence of a constant flux of mass, is possible due to the boundary conditions. We expect both the Navier conditions to be related to the presence of an open border in the system, that is, the deposited material that gets to the border leaves the system and never gets back into it. On the other hand, the Dirichlet conditions could be related to a system that is undergoing material drainage on the border, what could explain the quantitative differences among both sets of boundary conditions, such as the higher critical λ for the Dirichlet conditions. In any case, for a large enough λ no stationary solutions still exist, and this is due to the physical fact that the rate at which new material is entered into the system is simply too high and the system will be growing forever. In spite of the simplicity of our mathematical models, we still expect these predictions to be testable against suitable experiments. Indeed, the existence theory can be related to physical phenomena and therefore the validity of the models could be established, at least at a qualitative level.

Acknowledgements

This work has been supported by a grant provided by DST(SERB), New Delhi, India, File no. SB/S4/MS/805/12 and by the Government of Spain (Ministry of Economy, Industry and Competitiveness) through Project MTM2015-72907-EXP.

References

- [1] N. Anderson and A. M. Arthurs. Complementary variational principles for diffusion problems with michaelis-menten kinetics. *Bulletin of Mathematical Biology*, 42:131–135, 1980.
- [2] P. Balodis and C. Escudero. Polyharmonic k -hessian equations in \mathbb{R}^n . arXiv:1603.09392.
- [3] A.-L. Barabasi and H. E. Stanley. Fractal concepts in surface growth. *Cambridge University Press: Cambridge*, 1995.
- [4] C. Escudero. Geometric principles of surface growth. *Physical Review Letters*, 101:1–4, 2008.
- [5] C. Escudero, F. Gazzola, R. Hakl, I. Peral, and P. J. Torres. Existence results for a fourth order partial differential equation arising in condensed matter physics. *Mathematica Bohemica*, 140:385–393, 2015.
- [6] C. Escudero, F. Gazzola, and I. Peral. Global existence versus blow-up results for a fourth order parabolic pde involving the hessian. *J. Math. Pures Appl.*, 103:924–957, 2015.
- [7] C. Escudero, R. Hakl, I. Peral, and P. J. Torres. On radial stationary solutions to a model of nonequilibrium growth. *Euro. J. Applied Mathematics*, 24:437–453, 2013.
- [8] C. Escudero, R. Hakl, I. Peral, and P. J. Torres. Existence and nonexistence result for a singular boundary value problem arising in the theory of epitaxial growth. *Mathematical Methods in the Applied Sciences*, 37:793–807, 2014.
- [9] C. Escudero and E. Korutcheva. Origins of scaling relations in nonequilibrium growth. *Journal of Physics A: Mathematical and Theoretical*, 45:1–14, 2012.
- [10] C. Escudero and I. Peral. Some fourth order nonlinear elliptic problems related to epitaxial growth. *J. Differential Equations*, 254:2515–2531, 2013.
- [11] C. Escudero and P. J. Torres. Radial biharmonic k -hessian equations: The critical dimension. arXiv:1706.05684.
- [12] C. Escudero and P. J. Torres. Existence of radial solutions to biharmonic k -hessian equations. *J. Differential Equations*, 259:2732–2761, 2015.

- [13] Bruce A. Finlayson. *The Method of Weighted Residuals and Variational Principles*. Academic press, New York and London, 1972.
- [14] J. H. He. Variational iteration method a kind of nonlinear analytical technique:some examples. *Int. J. Non-Linear Mech.*, 34:699–708, 1999.
- [15] J. H. He. Variational iteration method : Some recent results and new interpretations. *J. Comput. Appl. Math.*, 207:3–17, 2007.
- [16] J. H. He and X. H. Wu. Variational iteration method: new development and applications. *Comput. Math. Appl.*, 54:881–894, 2007.
- [17] A. S. V. Ravi Kanth and K. Aruna. He’s variational iteration method for treating nonlinear singular boundary value problems. *Comput. Math. Appl.*, 60:821–829, 2010.
- [18] S. A. Khuri and A. Sayfy. A laplace variational iteration strategy for the solution of differential equations. *Appl. Math. Lett.*, 25:2298–2305, 2012.
- [19] V. F. Kirichenko and V. A. Krysko. Substantiation of the variational method in the theory of plates. *Int. Appl. Mech.*, 17:366–370, 1981.
- [20] R. K. Pandey and A. K. Verma. Existence-uniqueness results for a class of singular boundary value problems arising in physiology. *Nonlinear Anal.*, 9:40–52, 2008.
- [21] J. I. Ramos. On the variational iteration method and other iterative techniques for nonlinear differential equations. *Applied Mathematics and Computation*, 199:39–69, 2008.
- [22] T. E. Schunk. Zur knickfestigkeit schwach geklimr, ter zylindrlscher schalen. *Ing. Arch.*, 4:394–414, 1933.
- [23] M. Singh and A. K. Verma. An effective computational technique for a class of lane emden equations. *J. Math. Chem.*, 54:231–251, 2016.
- [24] M. Singh, A. K. Verma, and R. P. Agarwal. On an iterative method for a clas of 2 point and 3 point nonlinear sbvps. *Journal of Applied Analysis and Computation*, 9:1242–1260, 2019.
- [25] L. A. Soltani and A. Shirzadi. A new modification of the variational iteration method. *Comput. Math. Appl.*, 59:2528–2535, 2010.
- [26] A. M. Wazwaz. The variational iteration method for solving nonlinear singular boundary value problems arising in various physical models. *Commun. Nonlinear Sci. Numer. Simul.*, 16:3881–3886, 2011.
- [27] M. Zellal and K. Belghaba. An accurate algorithm for solving biological population model by the variational iteration method using he’ s polynomials. *Arab J. Basic Appl. Sci.*, 25:142–149, 2018.
- [28] X. Zhang, F. A. Shah, Y. Li, L. Yan, A. Q. Baig, and M. R. Farahani. A family of fifth order convergent methods for solving nonlinear equations usingvariational iteration technique. *J. Inform. Optim. Sci.*, 39:673–694, 2018.